Optimal configuration for the dual rotating-compensator Mueller matrix ellipsometer

Weichao Du [a], Shiyuan Liu [*, a, b], Chuanwei Zhang [b], and Xiuguo Chen [a]

[a] Wuhan National Laboratory for Optoelectronics, Huazhong University of Science and Technology, Wuhan 430074, China

[b] State Key Laboratory of Digital Manufacturing Equipment and Technology, Huazhong University of Science and Technology, Wuhan 430074, China

ABSTRACT

The dual rotating-compensator Mueller matrix ellipsometer based on the optical configuration $PC_{1r}(\omega_1)SC_{2r}(\omega_2)A$ has been developed recently with many applications such as characterization of thin film growth and surface modification. In this paper, the optimal configuration of this ellipsometer is performed by minimizing the condition number of the systematic data reduction matrix. We present the optimal orientation angles of the polarizer (P) and the analyzer (A), as well as the optimal number of sampling points and the optimal retardance of both compensators, and find that these optimal configurations at different frequency ratios of the two compensators (C_{1r} and C_{2r}) yield almost equal performance. Simulations conducted on this ellipsometer with different parameters have demonstrated that the optimal configuration improves the measurement accuracy.

Keywords: Mueller matrix ellipsometer (MME), Mueller matrix polarimeter, optimal configuration, condition number

1. INTRODUCTION

Several ellipsometers have been developed and applied as powerful tools for studying thin film growth and surface modification [1]. For anisotropic samples exhibiting inhomogeneities which lead to nonrandom depolarization or pseudo depolarization, more information is required to determine the sample parameters [2]. In this case, Mueller-Stokes formalism is used to describe 16 independent elements of the Mueller matrix of the sample, and complete studies require the development of ellipsometers able to measure all elements of the Mueller matrix of the sample [3]. In recent years, a number of Mueller matrix ellipsometer (MME) or Mueller matrix polarimeter (MMP) designs based on the configuration of coupled phase modulation components have been proposed. Compain and Drevillon described the design of an MME based on a coupled photoelastic modulator [4]. This design takes advantage of an easy-to-operate calibration method, and the high-frequency modulation of the four parameters of the polarization enables low-light-level measurements. Carcia-Caurel *et al.* used the coupled ferroelectric liquid crystal cell as the phase modulation in the MME and presented the spectroscopic measurements of a complete Mueller matrix with 1 nm resolution in the range from the visible to the near infrared [5]. Collions *et al*. described the design of a multichannel MME based on the dual rotating-compensator in the optical configuration $PC_{1r}(\omega_1)SC_{2r}(\omega_2)A$, which provided a real-time analysis of optically anisotropic materials [6-9]. Among these coupled configurations, the dual rotating-compensator MME provides the capability of determining a full unnormalized Mueller matrix with a wide spectrum region (1.5eV~6.5eV) [6].

In practice, error sources couple into the measurement and reduce the accurate reconstruction of the Mueller matrix for the MME. During the last decade, ellipsometer optimization has been widely discussed in the literature, most often in terms of the Stokes ellipsometer [10]. This ellipsometer optimization process guides the selection of polarization elements and their configurations to enhance stability in the presence of error sources. Sabatke *et al*. used the condition number and singular value decomposition to derive the optimal configurations for a rotating-compensator Stokes ellipsometer and performed the optimal compensator retardance when set at 132° [11]. Smith generalized these methods to an MME with a dual-rotating-retarder configuration and demonstrated that the optimal retardance must be equal to 127° compared to the 90° retarders generally used [12]. Carcia-Caurel *et al*. used the condition number to optimize the MME with liquid

* Contact author: shyliu@mail.hust.edu.cn; phone: +86 27 8755 9543; webpage: http://www2.hust.edu.cn/nom.

Eighth International Symposium on Precision Engineering Measurement and Instrumentation, edited by Jiubin Tan, Xianfang Wen, Proc. of SPIE
Vol. 8759, 875925 · © 2013 SPIE · CCC code: /13/$18 · doi: 10.1117/12.2014578

crystal retarders [13]. Twetmeyer and Chipman presented metrics related to the condition number and the singular value decomposition for optimizing the design of MME to ensure accurate reconstruction of a sample's Mueller matrix in the presence of error sources [14]. Most of these studies optimize mainly optical structural and parameters that make a large contribution to the condition number or optimal methods. However, there are other parameters, such as the number of sampling points, exerting an influence on the condition number. These parameters are defined by their authors and have not been discussed in detail. In this paper, we focus on these parameters that have not been discussed in detail and optimize the configuration of the dual rotating-compensator MME by minimizing the condition number of these parameters. Finally, we demonstrate that the optimal configuration has a low sensitivity to errors and improves the measurement accuracy.

The remainder of this paper is organized as follows. In Section 2 we reconstruct the original data analysis by Fourier analysis to a vector-vector dot product. Theoretical simulations are performed under variable parameters of the dual rotating-compensator MME in Section 3. Finally, we draw some conclusions in Section 4.

2. METHOD

2.1 System model of the dual rotating-compensator MME

The dual rotating-compensator MME considered in our work is based on the optical configuration $PC_{1r}(\omega_1)SC_{2r}(\omega_2)A$ as shown in Fig. 1, where P, S and A represent the polarizer, sample, and analyzer respectively. C_{1r} and C_{2r} are the synchronized rotating compensators with a frequency ratio ω_1:ω_2 of p:q, where p and q are integers.

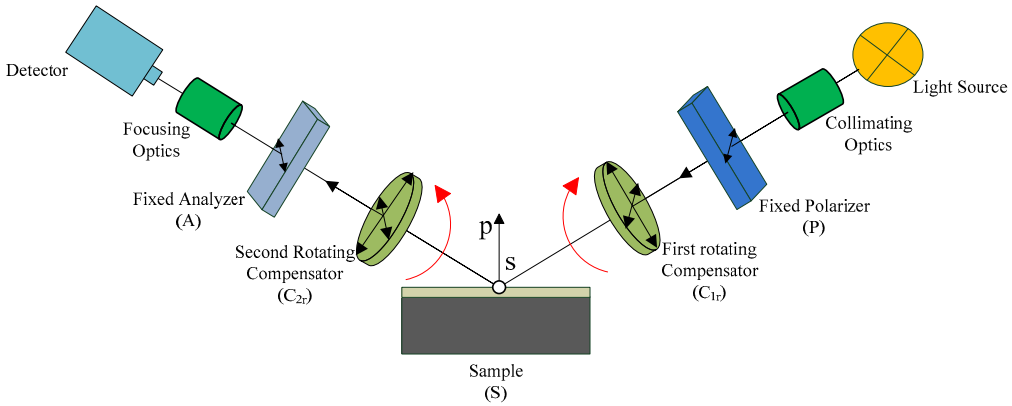

Fig.1. Schematic of dual rotating-compensator MME in the optical configuration $PC_{1r}(\omega_1)SC_{2r}(\omega_2)A$.

The optical signal is the dot-product of the first row of the total Mueller matrix of the configuration with the input Stokes vector. The detected waveform for this configuration is given as [8]:

$$I(t) = I_0 \left\{ 1 + \sum_{n=1}^{n_{\max}} \left[\alpha(2M_{2n}\omega)\cos(2M_{2n}\omega t - \varphi_{2n}) + \beta(2M_{2n}\omega)\sin(2M_{2n}\omega t - \varphi_{2n}) \right] \right\}, \quad (1)$$

where I_0 is the time-averaged irradiance (or dc Fourier coefficient), $(\alpha(2M_{2n}\omega), \beta(2M_{2n}\omega))$ are the normalized ac Fourier coefficients, ω is the base frequency, and φ_{2n} is the phase correction angle. Equation (1) employs the positive index n = 1, 2, ..., $n_{\max}$, which identifies the specific integer values M_{2n}, where M_{2n} is a signed integer index to be defined as a function of p and q below [8]. Particularly, the non-zero frequency $2M_{2n}\omega$ and the corresponding phases φ_{2n} must be bracketed pairs to highlight the symmetric roles of ω_1 and ω_2 in generating the $2M_{2n}\omega$ frequency component of $I(t)$ in Eq. (1). In addition, the ratio p:q must be defined to provide all Mueller matrix elements of the sample and maintain good stability in the rotation of both compensators. In this case, the 16 elements of the Mueller matrix ($m_{ij} = M_{ij}/M_{11}$; i = 1, 2, 3, 4; j = 1, 2, 3, 4) are able to be deduced by non-zero Fourier coefficients. We suggest that the reader refer to these works of Collins *et al.* for theory and details [6-9].

Since Eq. (1) is just the theoretical analysis for the waveform of the detected irradiances, the phase correction angle φ_{2n} must be determined using the instrument calibration. We start with an experimental expression for the irradiance waveform

$$I(t) = I_0' \left\{ 1 + \sum_{n=1}^{n_{\max}} \left[\alpha'(2M_{2n}\omega)\cos(2M_{2n}\omega t) + \beta'(2M_{2n}\omega)\sin(2M_{2n}\omega t) \right] \right\}. \tag{2}$$

When the instrument calibration is performed to extract the phase correction angle φ_{2n}, a transformation matrix must be used to determine the theoretical coefficients in Eq. (1). The $(\alpha'(2M_{2n}\omega), \beta'(2M_{2n}\omega))$ can be extracted during the data acquisition procedures from successive readouts of the multichannel detector. One readout is the integral of the irradiance waveform $I'(t)$ over 1/N of the k times optical period during the data acquisition procedure. It can be expressed as:

$$\begin{aligned} S_j &= \int_{(j-1)k\pi/N\omega}^{jk\pi/N\omega} I(t)dt \\ &= \frac{k\pi I_0'}{N\omega} + \sum_{n=1}^{n_{\max}} \frac{I_0'}{2M_{2n}\omega} \left(\sin\frac{kM_{2n}\pi}{N} \right) \times \left[\alpha'(2M_{2n}\omega)\cos\frac{(2j-1)kM_{2n}\pi}{N} + \beta'(2M_{2n}\omega)\sin\frac{(2j-1)kM_{2n}\pi}{N} \right] (j = 1, \ldots, N), \end{aligned} \tag{3}$$

where S_j is the measurement of optical flux of the detected light for the configuration, k is the multiple of the optical period in the data acquisition, and N is the number of sampling points for the waveform integrals in a k times optical period. Even numbered subscripts $2n$ are used here for consistency with previous work [6]. Equation (3) represents a system of N equations for unknown Fourier coefficients. Since the number of unknown Fourier coefficients is based on the value of (p, q) and is 25 at most, N must be more than 25 so that the equations are sufficient to deduce unknown Fourier coefficients.

2.2 Optimization metric of the dual rotating-compensator MME

The condition number is the metric used to optimize the configuration of the dual rotating-compensator MME. The goal of optimizing this MME is to minimize the condition number of the systematic data reduction matrix. Thus this approach will minimize the relative errors in Mueller matrix which result from uncertainties in calibration and measurement [9, 14]. For an arbitrary square matrix **A**, the condition number based on the L_p norm is defined as [15]:

$$cond(\mathbf{A}) = \| \mathbf{A} \|_p \| \mathbf{A}^{-1} \|_p, \tag{4}$$

where the notation $\| \mathbf{A} \|_p$ signifies the p-norm

$$\| \mathbf{A} \|_p = \sup_{x \in D(\mathbf{A})} \frac{\| \mathbf{Ax} \|_p}{\| \mathbf{x} \|_p} \quad \text{(matrix } p\text{-norm)}, \qquad \left(\| \mathbf{x} \|_p \right)^p = \sum_i x_i^p \quad \text{(vector } p\text{-norm)}, \tag{5}$$

where **x** is a vector, D(**A**) is the domain of **A,** and sup is the supremum. In this paper, $L_\infty (p = \infty)$ that is based on the maximum absolute column sum, is used to calculate the condition number.

Since Eq. (3) is the original data analysis for the dual rotating-compensator MME by Fourier analysis, it is disadvantageous for optimization studies. The independent relationship is exploited between these unknown Fourier coefficients and the Mueller matrix elements, and Eq. (3) is expressed as a vector-vector dot product form:

$$\mathbf{S}_j = \mathbf{W}_j \mathbf{M}, \tag{6}$$

where the Mueller matrix (**M**) is flattened into a 16×1 Mueller vector, and $\mathbf{W}_j$ (j = 1, ..., N) is the jth row of **W** that corresponds to a single sampling points measurement. **W** is typically determined from the data calibration and acquisition process. The Mueller matrix elements can be determined from Eq. (6). Generally, when N>16 the Mueller matrix **M** is over-determined. The pseudo-inverse matrix $\mathbf{W}_p^{-1}$ is used as the optimal data reduction equation for **M** and is mathematically equivalent to one performing a linear least-square fit.

$$\mathbf{M} = (\mathbf{W}^T \mathbf{W})^{-1} \mathbf{W}^T \mathbf{S} = \mathbf{W}_P^{-1} \mathbf{S}, \tag{7}$$

Thus, the condition number of the systematic data reduction matrix **W** is expressed by:

$$cond(\mathbf{W}) = \| \mathbf{W} \|_{\infty} \| \mathbf{W}_p^{-1} \|_{\infty} . \tag{8}$$

3. SIMULATIONS

Multiple simulations have been carried out for the dual rotating-compensator MME with different parameters including the polarizer and analyzer orientation angles, the number of sampling points (N) for waveform integrals, and the retardance of both compensators. In addition, the frequency ratio is determined based on the base frequency ω and the minimum scanning time of the detector. It must offer sufficient independent information to extract all Mueller matrix elements from the Fourier coefficients and avoid undesirable highest-order nonzero Fourier coefficients [6]. Hence, the different frequency ratios are defined as 5:1, 5:2, 5:3, and 5:4 in the simulations.

3.1 Simulation with varied number of sampling points *N*

Since the unknown Fourier coefficients are 25 at most in Eq. (3), the 26 sampling points of the waveform integrals are enough to deduce all $\left(I_0', \alpha'(2M_{2n}\omega), \beta'(2M_{2n}\omega)\right)$ theoretically [2,8]. If more points of waveform integrals in a single fundamental optical period are sampled, it would offer more information to describe the properties of the sample. However, the value of N is subject to the base frequency ω of the rotating compensators and the integration time of the detector. As a compromise between both of them, we obtain an optimal result as shown in Fig. 2. In the simulation, the polarizer and the analyzer have their transmission axes oriented horizontally. Both compensators have the same retardance, set at 127° [12], and orient their initial fast axes horizontally. Figure 2 shows that the distribution of the condition number varies with the value of N in a single fundamental optical period. The curves gradually become flat with increments of the value of N. We can obtain the optimal value equal to 72 at a frequency ratio equal to 5:3, and other frequency ratios yield almost equal performance. It is enough for us to obtain the 16 unknown elements of sample, and the condition number will not decrease with more points.

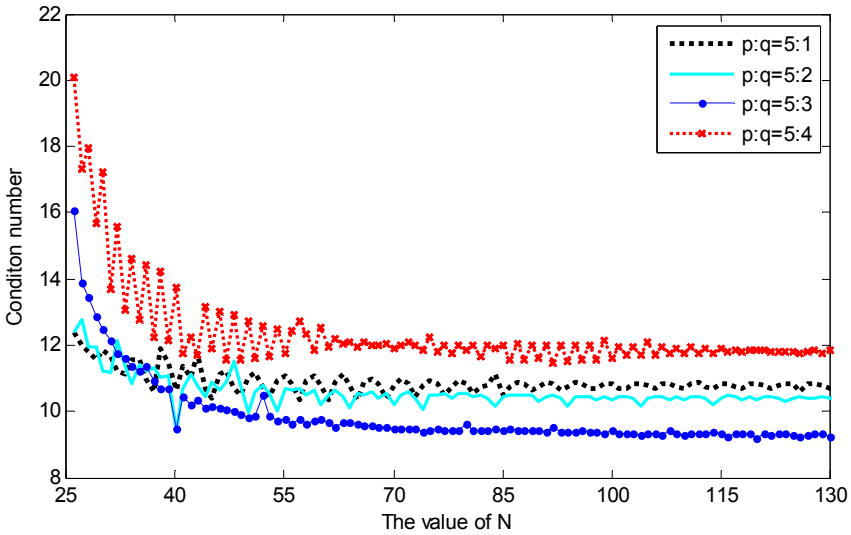

Fig. 2. Condition number of the data reduction matrix **W** for the dual rotating-compensator MME varies with the value of N for waveform integrals in a single fundamental optical period at different frequency ratios.

3.2 Simulation with varied orientation angles of polarizer and analyzer

The orientation angles of all optical elements (polarizer, compensators, and analyzer) are measured from the incident plane at a counterclockwise positive sense facing the source in the simulation. The retardance of both compensators is 127° with the horizontal orientation of the fast axes. The number of sampling points is 72. We can obtain some meaningful results shown in Fig. 3 based on the above conditions. Figure 3 shows how the condition number of the data reduction matrix **W** varies with the orientation angles of the polarizer and the analyzer at different frequency ratios. Though the condition number is the minimum at orientation angles of 0°, and 45°, this range shows a poor robustness. A

little shift of the orientation angle will lead to a great fluctuation of the condition number and will affect the reconstruction of **M**. The middle region is chosen due to its low condition number and its smoothness. Therefore, the optimal values of the orientation angles of the polarizer and the analyzer for the dual rotating-compensator MME are both 22°, resulting in a condition number of **W** equal to 17.8 in Fig. 3(c). It is noted that Figs. 3(a), 3(b), and 3(d) yield almost equal performance.

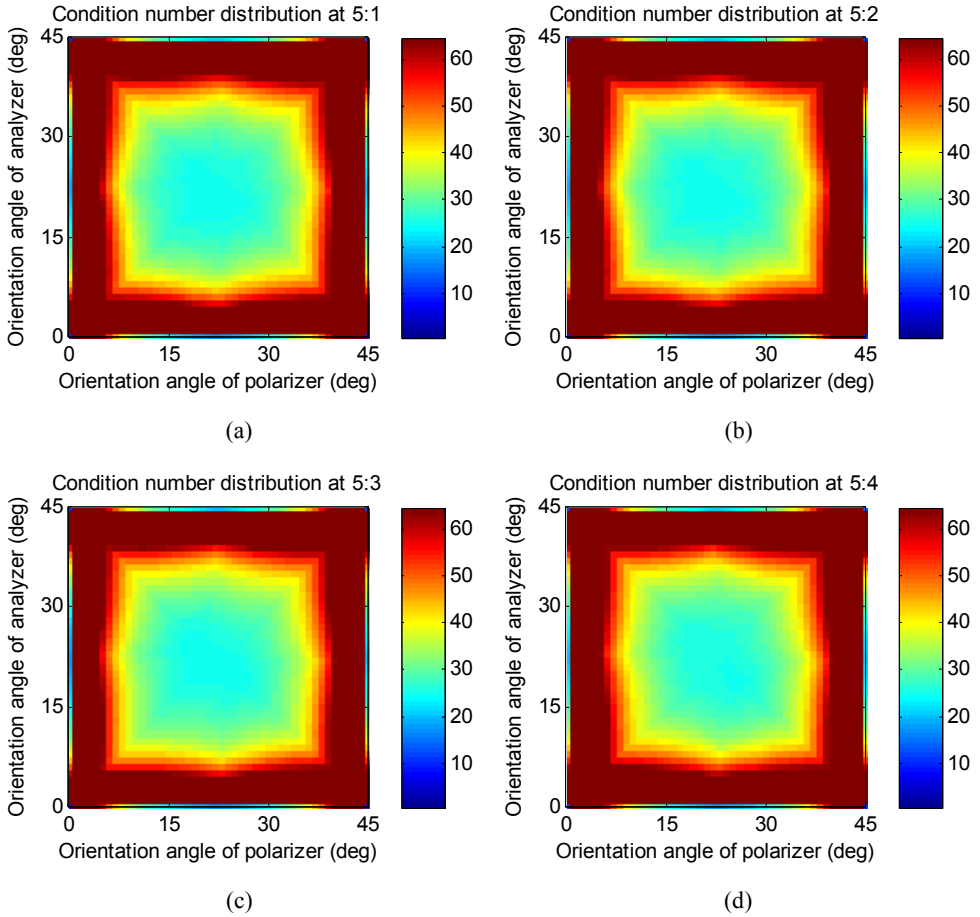

Fig. 3. The distribution of condition number operates independently increments of the orientation angles of the polarizer and the analyzer. (a), (b), (c), and (d) represent the different frequency ratios 5:1, 5:2, 5:3, and 5:4, respectively.

3.3 Simulation with varied retardance of both compensators

Compared to the quarter-wave generally used, Smith set the optimum retardance of both retarders at 127° in a simulation with a dual-rotating-retarder ellipsometer [12]. Here in our simulation, both compensators in the data reduction matrix are set to have the same retardance, and the initial orientations are set to be horizontal. The polarizer and analyzer have their transmission set at axis 22° from the incident plane. The sampling number is 72. Figure 4 shows how the condition number of the data reduction matrix **W** varied with the variable retardance. The minimum condition number can be obtained at 110° with the frequency ratio 5:3, and the curve is flat in the region of 110°. Thus the optimal retardance of both compensators is 110°. Other frequency ratios yield the same performance.

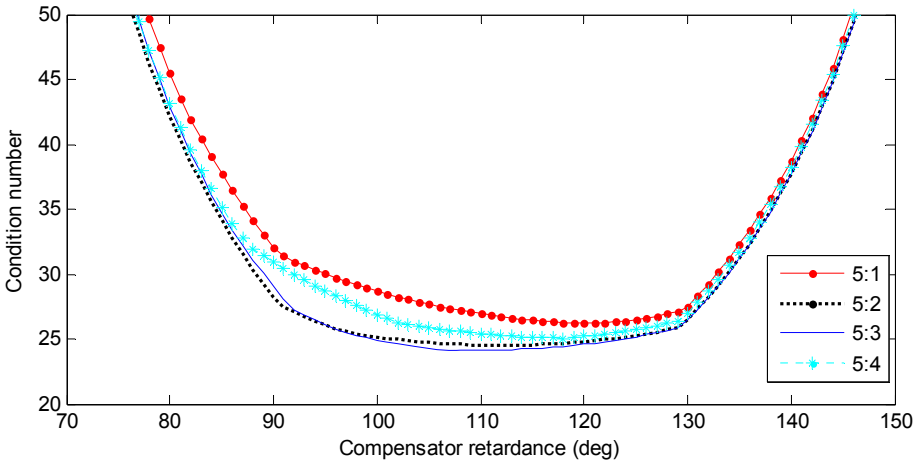

Fig. 4. The condition number as a function of the retardance of both compensators for the MME. The optimum value is a retardance of 110° with the frequency ratio 5:3.

3.4 Simulation with random noise

In this section, random noise due to unstable rotating errors of both compensators is considered in order to test the error sensitivity of the Mueller matrix under different conditions. The sample is defined as air with the Mueller matrix as:

$$\mathbf{M} = \begin{pmatrix} 1.000 & 0 & 0 & 0 \\ 0 & 1.000 & 0 & 0 \\ 0 & 0 & 1.000 & 0 \\ 0 & 0 & 0 & 1.000 \end{pmatrix}.$$

The simulation is performed with the same random noise under three different conditions. The orientation angles of all optical elements (polarizer, compensators, and analyzer) are measured from the incident plane at a counterclockwise positive sense facing the source in the simulation. The frequency ratio is defined as 5:3, and both compensators orient the fast axes horizontally. In condition 1, the retardance of both compensators is 127° (θ_1=θ_2=127°) which is optimized by Smith [12]. The polarizer orientation is 0° (P'=0°), the analyzer orientation is 10° (A'=10°), and N=36. In condition 2, the optimal configurations are defined based on the results we have obtained (P'=22°, A'=22°, N=72, θ_1=θ_2=110°). In condition 3, the retardance is defined as the quarter-wave which is generally used (θ_1=θ_2=90°). Other parameters are set as P'=22°, A'=12°, and N=28. Figure 5 shows that the Mueller matrix is not sensitive to random noise in condition 2. Since the first element of the Mueller matrix is normalized in the calculation [2], it is not presented in the figure. The simulation demonstrates that the measurement accuracy is improved based on the optimal configuration.

4. CONCLUSIONS

In this paper, this study has presented an optimization analysis of a dual rotating-compensator MME. It is found that the optimal number of sampling points and the orientation angles of the polarizer and the analyzer are 72 and 22°, respectively, and the optimal retardance of both compensators is 110°. In addition, different frequency ratios do not have an obvious influence on the simulation, and results yield almost equal performance. Finally, it demonstrates that the optimal configuration has a low sensitivity to errors and improves the measurement accuracy. It is expected that this study could be applicable to optimizing the configuration of the dual-rotating compensator MME.

ACKNOWLEDGMENT

The authors wish to acknowledge the financial support from the National Natural Science Foundation of China (Grant No. 91023032, 51005091) and the National Instrument Development Specific Project of China (Grant No. 2011YQ160002).

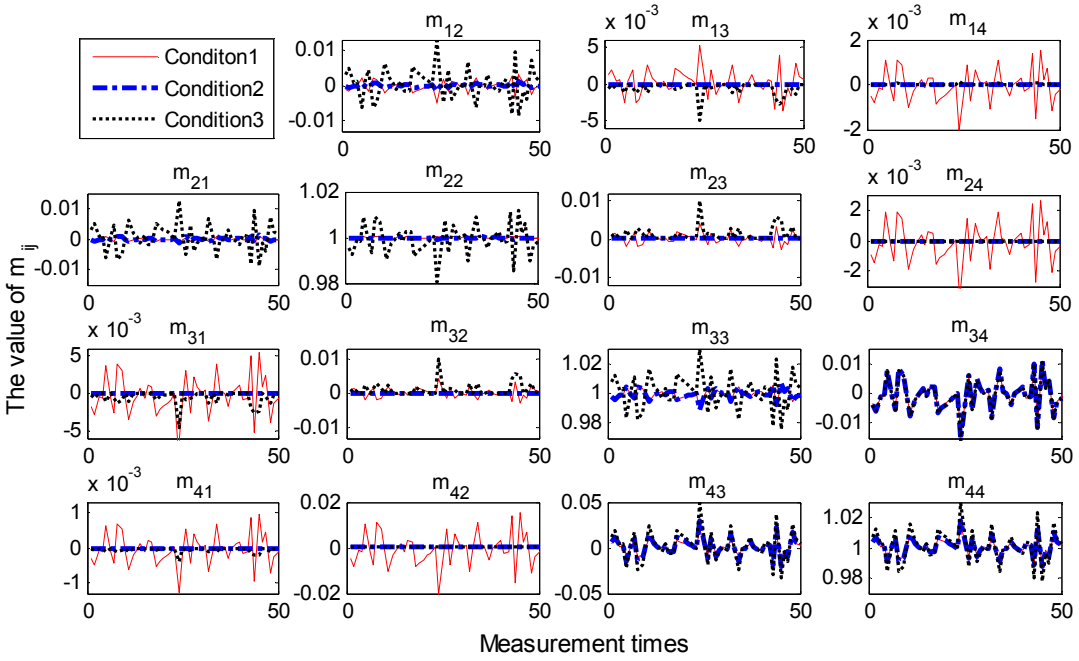

Fig. 5. Measurement errors of the perfect air sample are performed with three different conditions. The first element of Mueller matrix m_{11} is normalized to 1, and is not presented in the figure.

REFERENCES

[1] H. Fujiwara, [Spectroscopic Ellipsometry Principles and Applications], Maruzen Co. Ltd, Tokyo, 87-113 (2007).

[2] H. G. Tompkins and E. A. Irene, [Handbook of Ellipsometry], William Andrew, New York, 246-251 (2005).

[3] L. Broch, A. E. Nacir, and L. Johann, "Sysmatic errors for a Mueller matrix dual rotating compensator ellipsometer," Opt. Express **16**, 8814-8824 (2008).

[4] E. Compain and B. Drevillon, "Complete high-frequency measurement of Mueller matrix based on a new coupled-phase modulator," Rev. Sci. Instrum. **68**, 2671-1680 (1997).

[5] E. Garcia-Caurel, A. D. Martina, and B. Drevillon, "Spectroscopic Mueller polarimeter based on liquid crystal devices," Thin Solid Films **455-456**, 120-123 (2004).

[6] R. W. Collins and J. Koh, "Dual rotating-compensator multichannel ellipsometer: Instrument design for real-time Mueller matrix spectroscopy of surfaces and films," J. Opt. Soc. Am. A **16**, 1997-2006 (1999).

[7] C. Chen, I. An, G. M. Ferreira, N. J. Podraza, J. A. Zapien, and R. W. Collins, "Multichannel Mueller matrix ellipsometer based on the dual rotating compensator principle," Thin Solid Films **455-456**, 14-23 (2004).

[8] J. Li, B. Ramanujam, and R. W. Collins, "Dual rotating compensator ellipsometry: Theory and simulations," Thin Solid Films **519**, 2725-2729 (2011).

[9] J. Lee, J. Koh, and R. W. Collins, "Dual rotating-compensator multichannel ellipsometer: Instrument development for high-speed Mueller matrix spectroscopy of surfaces and thin films," Rev. Sci. Instrum. **72**, 1742-1754 (2001).

[10] R. A. Chipman, [Handbook of Optics, 2nd ed.], McGraw-Hill, New York, 22.1-22.37 (1995).

[11] D. S. Sabatke, M. R. Descour, E. L. Dereniak, W. C. Sweatt, S. A. Kemme, and G. S. Phipps, "Optimization of retardance for a complete Stokes polarimeter," Opt. Lett. **25**, 802-804 (2000).

[12] M. H. Smith, "Optimization of a dual-rotating-retarder Mueller matrix polarimeter," Appl. Opt. **41**, 2488-2493 (2002).

[13] E. Garcia-Caurel, A. D. Martin, and B. Drevillon, "Optimized Mueller polarimeter with liquid crystals," Opt. Lett. **28**, 616-618 (2003).

[14] K. M. Twetmeyer and R. A. Chipman, "Optimization of Mueler matrix polarimeters in the presence of error sources," Opt. Express **16**, 11589-11603 (2008).

[15] R. D. Skeel and J. B. Keiper, [Elementary Numerical Computing with Mathematica], McGraw-Hill, New York, 124-126 (1993).